Engineering Journal issn: 0125-8281

Article

Flexural Response of CFRP-Strengthened Steel Beams with Initial Bond Defects

Tosporn Prasertsri[a], Akhrawat Lenwari[b,*], and Thaksin Thepchatri[c]

Composite Structures Research Unit, Department of Civil Engineering, Faculty of Engineering, Chulalongkorn University, Bangkok 10330, Thailand
E-mail: [a]tosporn.p@student.chula.ac.th, [b]akhrawat.l@chula.ac.th (Corresponding author), [c]thaksin.t@chula.ac.th

Abstract. This paper presents the flexural behavior of steel beams strengthened with partial-length adhesive-bonded carbon fiber-reinforced polymer (CFRP) plates under static four-point bending. An initial bond defect was intentionally introduced in the constant moment region of the CFRP-strengthened steel beams. In the experimental program, the test variables included the size of the initial bond defect, FRP modulus, FRP plate length, and condition of the steel beam before installation of the FRP plate (undamaged and pre-yielded conditions). Based on the test results, the presence of the initial bond defect changed the failure mode of FRP-strengthened steel beam from the fiber rupture to intermediate plate debonding. With the initial bond defect, the effectiveness of the FRP strengthening scheme decreased as FRP modulus increased. The stiffness, strength, and ductility index of the CFRP-strengthened beam with the initial bond defect decreased as the defect size increased. However, the initial bond defect had no detrimental effect on the maximum load capacity and ductility index of the strengthened beams. The strengthening effectiveness in terms of stiffness, strength, and ductility enhancement was more pronounced in the case of the pre-damaged steel beam, of which the bottom flange had already yielded before installation of the CFRP plate, than the undamaged steel beam.

Keywords: Fiber-reinforced polymer, flexural strengthening, initial bond defect, steel beam, debonding.

ENGINEERING JOURNAL Volume 24 Issue 1
Received 6 July 2019
Accepted 9 December 2019
Published 8 February 2020
Online at http://www.engj.org/
DOI:10.4186/ej.2020.24.1.115

DOI:10.4186/ej.2020.24.1.115

1. Introduction

Use of fiber-reinforced polymer (FRP) materials for strengthening steel structures has been widely recognized due to their high mechanical properties and lightweight [1-5]. The FRP strengthening is superior to steel jacketing since no residual stress due to a welding process is induced. It is recommended for beams in chemical plants or oil storage tanks where a welding process must be avoided [6]. Previous research works have investigated the effectiveness of the externally-bonded FRP plates on strengthening steel beams [7-9]. Various analysis methods such as the principle of virtual work [8], nonlinear finite element analysis [10-13], and closed-form analytical solutions [9, 14, 15] have been proposed to predict the flexural behavior of the FRP-strengthened steel beams. Schnerch et al. [7] conducted a four-point bending test on steel beams strengthened with high modulus carbon fiber-reinforced polymer (CFRP) plates using different adhesives. The test results showed that the failure mode of the strengthened steel beam depends on the type of adhesive and FRP length. Possible failure modes include the fiber rupture and plate debonding. Debonding is a premature failure because the FRP plate is not utilized to the full tensile strength. Lenwari et al. [8] examined the effects of the FRP length on the flexural behavior of strengthened steel beams. The study concluded that the failure mode was fiber rupture in case of the long FRP plate. The plate debonding occurred in case of the short FRP plate. The plate debonding initiated at the termination point of the FRP plate and propagated towards midspan. Another failure mode is the intermediate debonding of the FRP plate. The intermediate debonding starts within the beam span and propagates towards the plate end [11, 16-18]. It may occur due to yielding of the steel beam or the presence of bond defects [17]. The debonding process is more gradual than plate end debonding [19]. In practice, the imperfections between the FRP strengthening system and the steel beam can be in the form of notches [12, 15, 18, 20] and bond defects [15-17]. Some previous studies [21-27] have utilized an anchorage system to prevent the FRP debonding failure in the FRP-strengthened steel and reinforced concrete (RC) beams. In the FRP-strengthened RC beams, the anchorage system was used to increase the FRP debonding strain [28]. Also, a combined use of glass FRP and CFRP laminates was proposed [29]. Using the anchorage systems, some tested steel and RC beams still failed due to FRP debonding [22, 24, 30, 31]. From a literature review, the research works that investigated the effects of initial bond defects on the flexural response of CFRP-strengthened steel beams have been limited [16, 17, 19].

This research examines the effects of initial bond defects on the flexural responses of CFRP-strengthened steel beams. Effects of FRP modulus, FRP plate length, and condition of the steel beam before installation of the FRP plate (undamaged and pre-yielded conditions) are also investigated using a four-point bending test. The examined flexural properties include stiffness, strength, and ductility of the FRP-strengthened beams.

2. Experimental Program

In the experimental program, the test variables included the size of an initial bond defect, CFRP modulus, length of the CFRP plate, and condition of the steel beam before installation of the CFRP plate (undamaged and pre-damaged conditions). Table 1 describes the tested steel beams. One steel beam without CFRP strengthening system was used as the control beam (CB), as shown in Fig. 2. Five beams were strengthened with Sika® CarboDur®M514 (BM) and two beams were strengthened with Sika® CarboDur®S512 (BS). The span length was 1.80 m. The CFRP lengths were 1.20 and 1.50 m, respectively. The notation "Y" indicates the occurrence of yielding at the midspan bottom flange before attaching the CFRP plate. This simulated the repair condition where severe service distress had already occurred in the beams. A numeric value "2a" after the symbol "-" denotes the length of an initial bond defect (mm) at the midspan. The cross sections of tested beams are shown in Fig. 1. A hot-rolled wide-flange section W150 14.0 kg/m was used. Steel cover plates (300 mm wide by 12 mm thick) were welded to the top flanges of steel beams to prevent compression yielding. The nominal thicknesses (t_{frp}) of Sika® CarboDur®M514 and Sika® CarboDur®S512 plates were 1.4 mm and 1.2 mm, respectively. The adhesive layer thickness (t_{adh}) was 3.5 mm.

Refer to Lenwari et al. [8], the plate length of at least 1.20-m was chosen to avoid the plate end debonding failure. A pilot steel beam BM120-100 was tested until failure due to intermediate debonding. At the maximum applied load, the measured bottom flange strain at midspan section was 1.7%, which was approximately 9.7 times the yield strain of the steel beam. The pre-loading was released before the CFRP installation. Note that the pilot steel beam BM120-100 is not beam BM120-100 shown in Table 1.

2.1. Material Properties

Figure 3 shows the static test setup for tensile properties of steel and CFRP materials. The steel coupons were cut from flat regions of the flange of wide-flange beams as in ASTM A370 [32]. The tensile properties of steel included yield stress, yield strain, and elastic modulus. Rupture stress and elastic modulus of CFRP coupons were obtained from the identical test. All coupon specimens were tested under displacement control at a rate of 1mm/min until failure.

Table 2 shows the tensile properties of steel and CFRP plates. Note that E is elastic modulus, σ_y is yield stress of steel, and σ_{fu} is tensile stress of CFRP plate. The tensile strength of steel coupon is defined as σ_u. Tensile properties of SikaDur®-30 are based on the manufacturer data [33]. The elastic modulus and tensile

stress of SikaDur®-30 is 11,200 MPa and 31 MPa, respectively. Many works [34-40] showed that the variation of properties was relatively low.

Table 1. Details of tested steel beams.

Beam	CFRP type	CFRP plate length (mm)	Predamage	*2a* (mm)
CB	-	-	-	-
BM120-0	Sika® CarboDur®M514	1,200		
BM120-50				50
BM120-100				100
BM120Y-100			Yes	
BM150-100		1,500	-	
BS120-0	Sika® CarboDur®S512	1,200		-
BS120-100				100

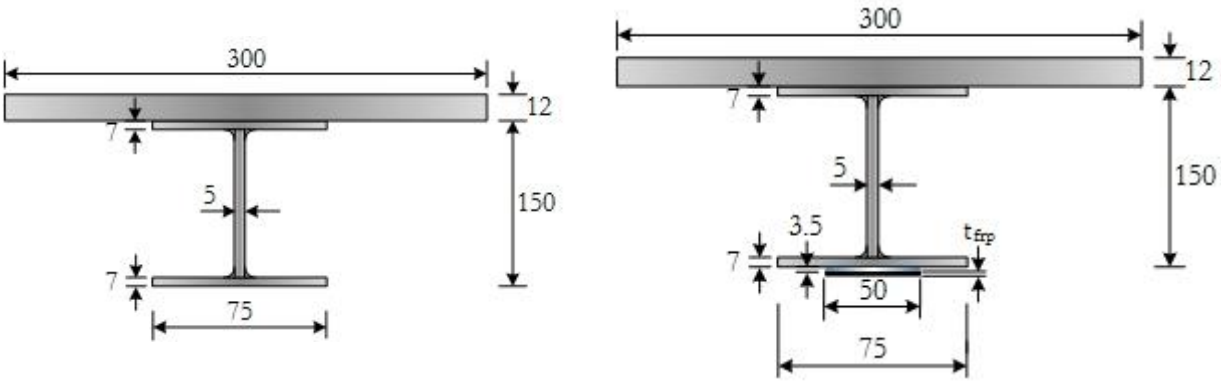

(a) Control steel beam (b) FRP-strengthened steel beams

Fig. 1. Cross sections of tested beams (all dimensions in mm).

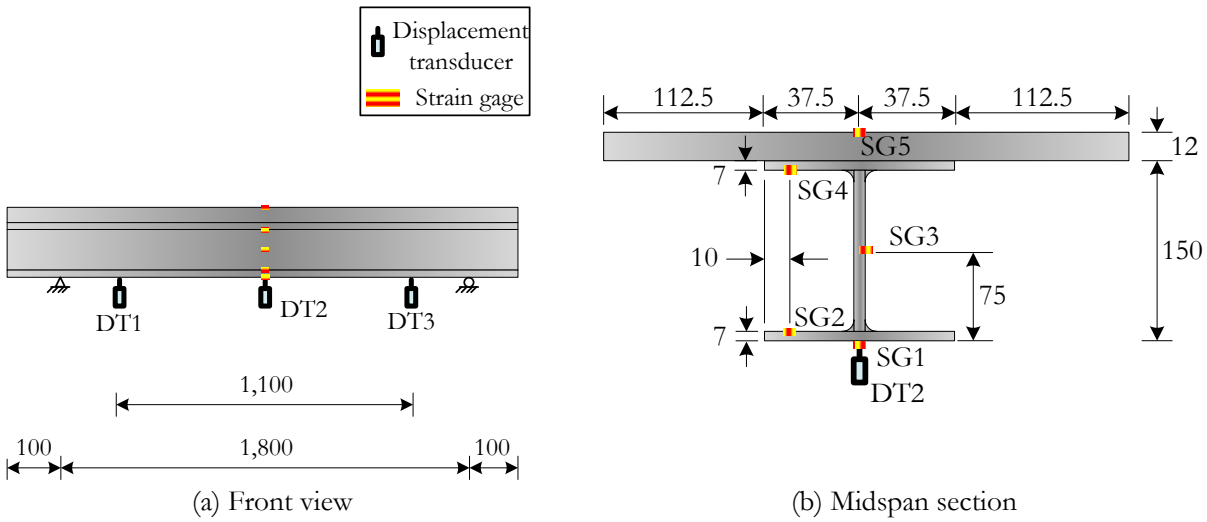

(a) Front view (b) Midspan section

Fig. 2. Instrumentation for control (unstrengthened) steel beam (all dimensions in mm).

DOI:10.4186/ej.2020.24.1.115

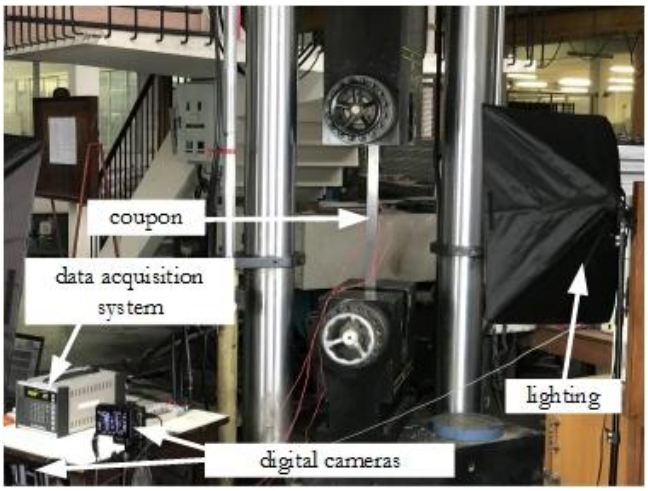

Fig. 3. Tensile testing of coupons.

Table 2. Tensile properties of steel and CFRP plates.

Material	E (MPa)	σ_y (MPa)	σ_u or σ_{fu} (MPa)
Steel beam	178,091	318	458
Steel plate	182,590	284	397
Sika® CarboDur® S512	180,777	-	3,303
Sika® CarboDur® M514	238,575	-	2,522

2.2. Initial Bond Defects

In this study, the bottom flange surface of steel beams was prepared by SA3 sandblasting (blast-cleaning to visually clean steel condition). This process was classified according to ISO 8501-1 [41]. Then, the CFRP plate was adhesively bonded within three hours after sandblasting of the bottom flange surface to avoid the contamination from either dirt or rust. The adhesive curing time was 30 days to ensure the bond between FRP and the steel substrate.

An initial bond defect at the steel-adhesive interface was introduced using the polyester film-based insulation paper as shown in Fig. 4. The thickness and length of insulation paper were 0.25 mm and 100 mm, respectively. An insulation paper was folded and temporally affixed on the steel surface using a transparent tape. The width of the insulation paper varied from 50 to 100 mm in order to create the initial bond defect. The polyester film was slippery. This simulated the unbonded condition at the steel-adhesive interface. The insulation paper was positioned at the bottom flange of the steel beam at midspan before the installation of CFRP plates.

2.3. Test Setup and Instrumentation

A static flexural test was conducted under four-point bending as shown in Fig. 5. A 300-kN capacity hydraulic jack was used to apply the load using the spreader steel beam. The applied loads were transmitted through the steel rollers at bottom of the spreader steel beam. The spacing between two applied loads was 150 mm. The tested beams were placed on the roller supports, which allow the beams to behave in a simply supported manner. The test was carried out under displacement control until failure. The rate of midspan deflection was controlled at 1 mm/min.

Electrical resistance strain gages were installed to measure the strain distribution along the section height of beam CB, as shown in Fig. 2. Strain gages and displacement transducers are denoted by "SG" and "DT", respectively. SG1 located at the bottom surface of the bottom flange, and SG2 was installed at the upper surface of the bottom flange. SG3 and SG4 located at mid-height of the W150×75 section and the bottom surface of the top flange, respectively. The compressive strain at top surface of the steel cover plate was measured by SG5. Three displacement transducers measured the deflections at midspan and locations near the CFRP plate terminations.

For FRP-strengthened steel beams, the FRP strains were measured with nineteen strain gages as shown in Fig. 6. Thirteen of them were attached on the CFRP plate. The other six were installed on the steel beam and cover plate.

Figure 7(a) shows the strain gage locations for FRP-strengthened steel beams. SG1, SG2, SG18, and SG19 were used to detect the debonding near the plate ends,

while SG3-SG6, SG13, SG15-SG17 were used to detect the intermediate debonding. SG8 was used for the FRP tensile strain at midspan. The bottom flange yielding within the initial bond defect zone was observed from three strain gages SG7, SG9, and SG14 at the steel bottom flange. Additional strain gages were also installed to measure the strain distribution across the midspan section, as shown in Fig. 7(c). However, typical strain signals for the detection of steel yielding, fiber rupture, and intermediate debonding will be presented in the paper.

For the unstrengthened steel beam (beam CB), the test was terminated when the compressive strain at the steel cover plate reached 75% of yield strain of the steel plate. Tensile strain at the bottom flange was about 1.97%, which is approximately 11 times the yield strain of the steel beam. The test on FRP-strengthened steel beams was terminated when FRP rupture or debonding occurred. The applied loads rapidly decreased before the global failure of the beam. The maximum midspan deflection was defined by the midspan deflection at the maximum load. Strain, deflection, and applied load values were recorded with a data logging system during the test. A dual sampling rate was chosen. A 100 Hz sampling rate was selected to capture an abrupt event triggered by fiber rupture and intermediate debonding. A sampling rate of 5 Hz was used for the investigation of static behavior of tested beams.

(a) Polyester film-based insulation paper

(b) Paper position at bottom flange

(c) CFRP plate installation

(d) Removal of excess paper

Fig. 4. Creation of initial bond defect.

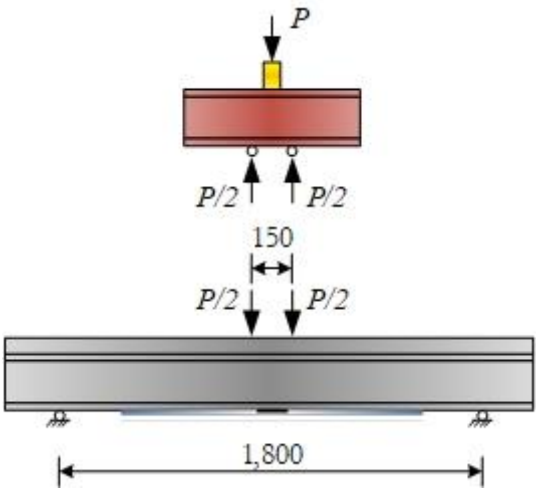

(a) Loading condition

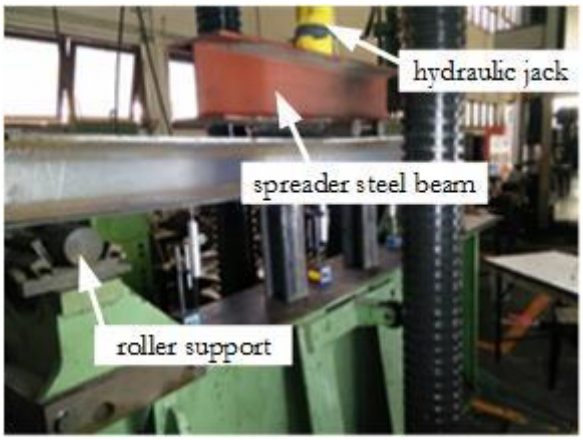

(b) Instrumentation

Fig. 5. Test setup for tested beams (static four-point loading scheme).

DOI:10.4186/ej.2020.24.1.115

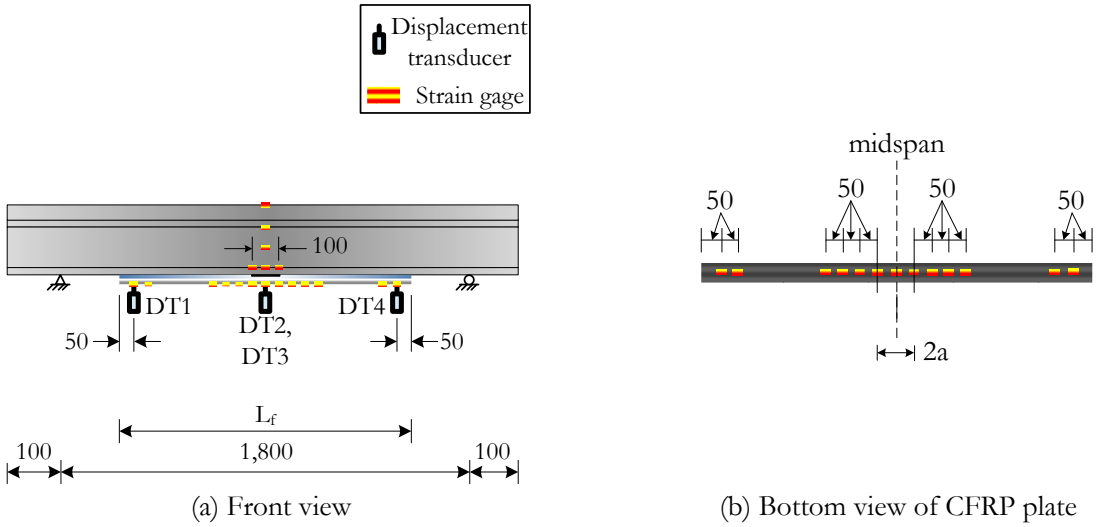

(a) Front view (b) Bottom view of CFRP plate

Fig. 6. Instrumentation on FRP-strengthened steel beams (all dimensions in mm).

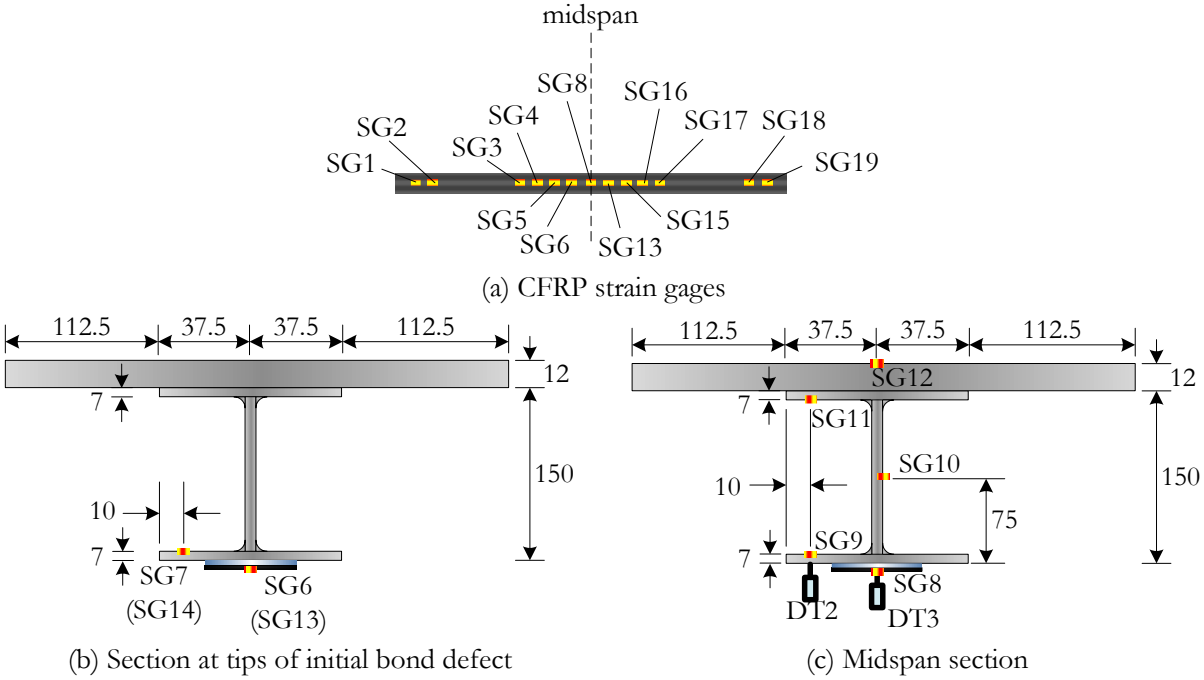

(a) CFRP strain gages

(b) Section at tips of initial bond defect (c) Midspan section

Fig. 7. Details of instrumentation on CFRP plate and steel beam (all dimensions in mm).

3. Experimental Results

Table 3 summarizes the static test results of all tested beams. The flexural properties include the midspan deflection at yield load (Δ_y), yield load (P_y), midspan deflection at maximum load (Δ_{max}), and maximum load capacity (P_{max}). The yielding of steel beams refers to the state when upper surface of the bottom flange yielded. The secant stiffness is defined as the ratio between P_y and Δ_y. The ductility index is defined as the ratio between Δ_{max} and Δ_y.

Four displacement transducers were installed to measure the deflection at midspan and points near the plate ends, as shown in Fig. 8. Two transducers were affixed at the midspan. One of them was pointed to the lower surface of the bottom flange and the other one to the FRP plate. The midspan deflection was based on the transducer pointed to the lower surface of the bottom flange.

A video camera recording in slow-motion at 1,000 frames per second was used to capture the time when failure occurred in the FRP-strengthened steel beams. The fiber rupture occurred in strengthened beams with no bond defect, while the intermediate debonding occurred in strengthened beams with an initial bond. Fig. 9(a) shows the failure of beam BM120-0 which is a typical fiber rupture (FR) failure. Some broken carbon fiber pieces detached from the FRP plate as depicted in

Fig. 10(a). Figure 9(b) shows the failure of beam BM150-100 which is a typical intermediate debonding (ID) failure. There is no evidence of broken carbon fiber pieces detached from the FRP plate. Some portions of the FRP plate were adhered at the lower surface of bottom flange, as shown in Fig. 10(b).

Figure11 shows typical strain gage signals for detection of the steel yielding, fiber rupture, and intermediate debonding. It can be seen that yielding of the steel beam occurred before fiber rupture and intermediate debonding. The cracking sound occurred at the time when the first fiber breaking of the CFRP plate was detected. In case of the intermediate debonding, the FRP strain suddenly dropped after debonding.

Table 3. Flexural properties of tested steel beams.

Beam	Δ_y (mm)	P_y (kN)	Stiffness (kN/m)	Δ_{max} (mm)	P_{max} (kN)	Δ_{max} / Δ_y	Failure mode*
CB	4.95	98.3	19,865	19.92	132.5	4.03	BFY
BM120-0	4.44	96.1	21,647	14.64	163.1	3.30	FR
BM120-50	3.77	85.6	22,720	18.75	191.0	4.98	ID
BM120-100	4.51	87.1	19,287	17.39	163.9	3.85	ID
BM120Y-100	5.24	120.5	22,985	24.51	198.7	4.68	ID
BM150-100	4.55	98.5	21,654	16.39	182.5	3.60	ID
BS120-0	4.51	89.5	19,846	23.60	182.1	5.23	FR
BS120-100	3.97	79.3	19,957	33.52	200.3	8.44	ID

Remark * BFY = Bottom Flange Yielding; FR = Fiber Rupture; ID =Intermediate Debonding.

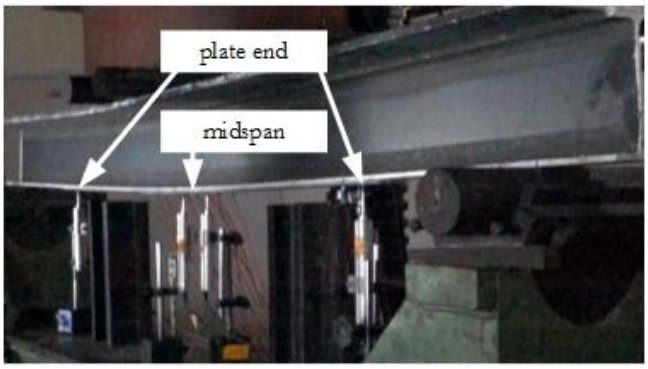

Fig. 8. Beams specimens during static testing.

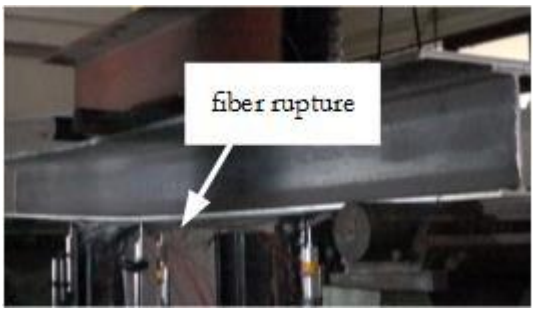

(a) Fiber rupture (beam BM120-0)

(b) Intermediate debonding (beam BM150-100)

Fig. 9. Failure modes of CFRP-strengthened steel beams.

DOI:10.4186/ej.2020.24.1.115

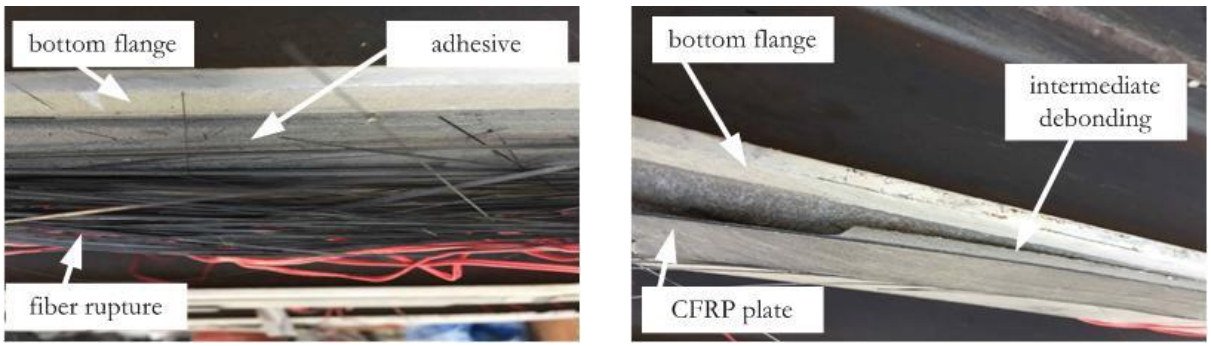

(a) Fiber rupture (beam BM120-0) (b) Intermediate debonding (beam BS120-100)

Fig. 10. Close-up view of failure modes of CFRP-strengthened steel beams.

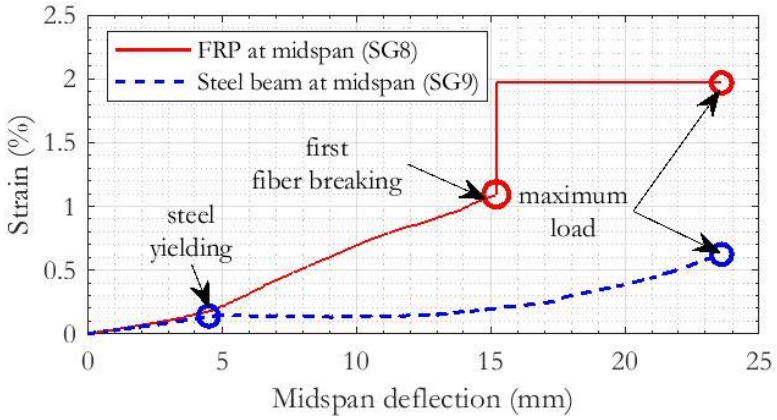

(a) Fiber rupture mode (beam BS120-0)

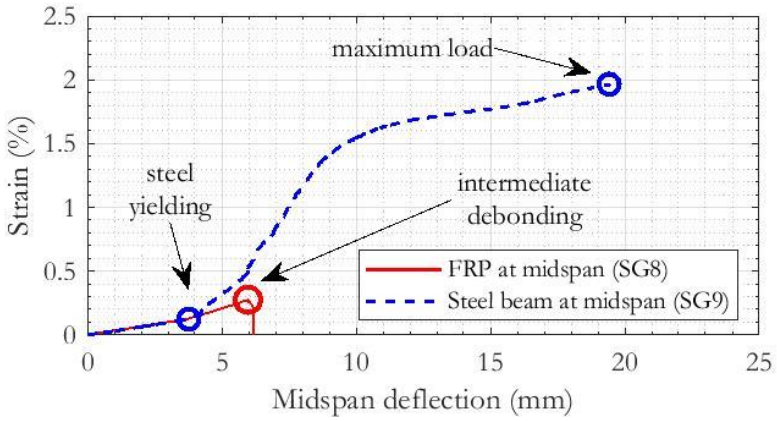

(b) Intermediate debonding mode (beam BM120-50)

Fig. 11. Typical strain gage signals for detection of steel yielding, fiber rupture, and intermediate debonding.

3.1. Effect of FRP Modulus on Flexural Properties

Figure 12 shows the load-deflection relationships of the control beam and CFRP-strengthened beams. Without an initial bond defect, an increase in FRP modulus improved the stiffness of the strengthened beams by 9%, but decreased the strength and ductility index by 10% and 37%, respectively. With an initial bond defect, the effect of FRP modulus on the stiffness was minimal. However, the strength and ductility index of the strengthened beams decreased by 18% and 54%, respectively, when FRP modulus increased (by 32%). Therefore, the detrimental effect of FRP modulus on the strength and ductility of FRP-strengthened steel beams increased due to the presence of an initial bond defect.

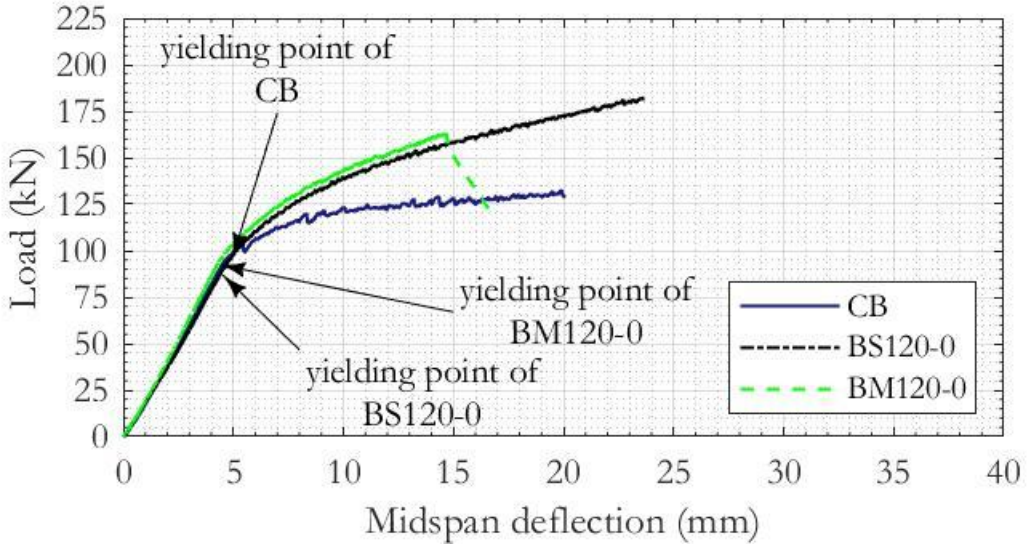

(a) FRP modulus (no bond defect)

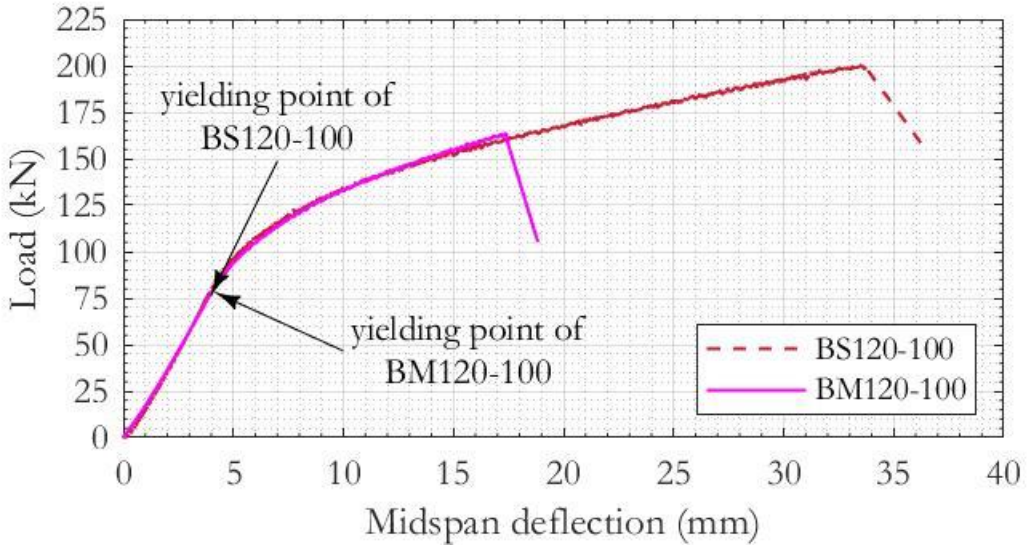

(b) FRP modulus (with bond defect)

Fig. 12. Effect of FRP modulus on load-deflection curve.

3.2. Effect of Initial Bond Defect Length on Flexural Properties

Figure 13 compares the load-deflection relationships of CFRP-strengthened steel beams containing an initial bond defect of different lengths (about 4-8% of FRP length). In case of low FRP modulus, the effect of initial bond defect length on the stiffness was minimal. When there was an initial bond defect, i.e., the FRP plate was not perfectly bonded to the steel beam, the yield load decreased by 9-11%. However, the initial bond defect improved the strength and ductility of the strengthened beams. The maximum load capacity was enhanced by 10-17% compared to the capacity of the beam without an initial bond defect. The ductility index was also increased by 17-61%. Possibly, the strain in FRP plate was reduced because some parts of the FRP plate within the maximum moment zone was not fully bonded to the steel beam. These findings are consistent with Choi et al. [42] who reported that the load capacity of the strengthened beam increased when the length of bond defect increased.

3.3. Effect of FRP Plate Length on Flexural Properties

Figure 14 compares the load-deflection relationships of CFRP-strengthened steel beams using different plate lengths. It can be seen that strength and stiffness of the strengthened beam increased as FRP length increased. In this study, an increase in FRP length of 25% increased the maximum load capacity by 11%, while it decreased the ductility index by 6%.

DOI:10.4186/ej.2020.24.1.115

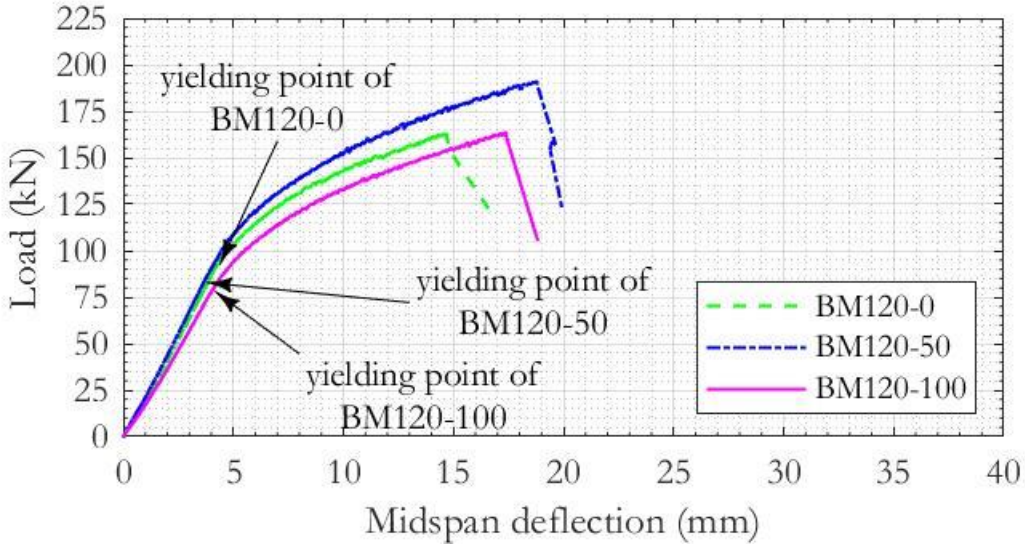

(a) initial bond defect length (beam strengthened with Sika® CarboDur® M514)

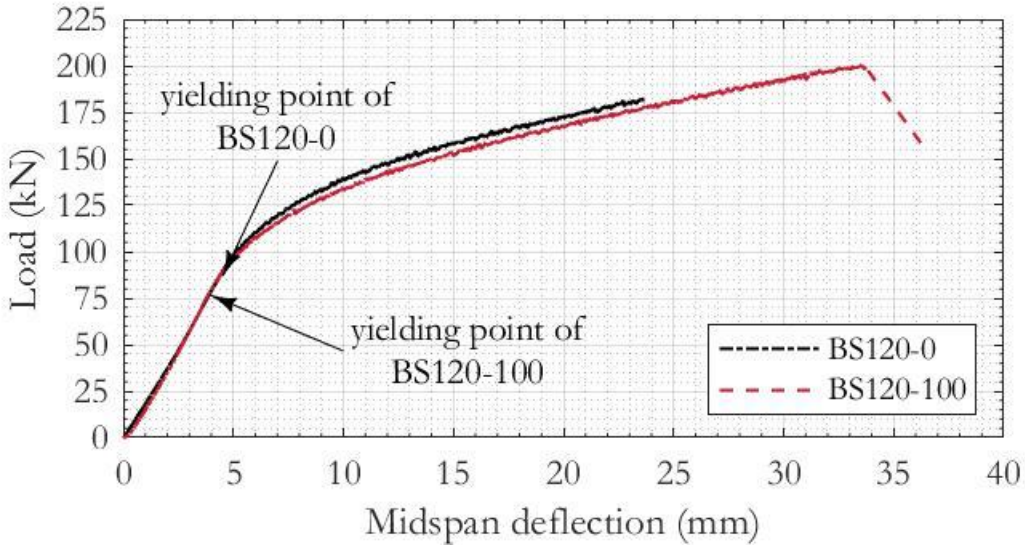

(b) initial bond defect length (beam strengthened with Sika® CarboDur® S512)

Fig. 13. Effect of initial bond defect on load-deflection curve.

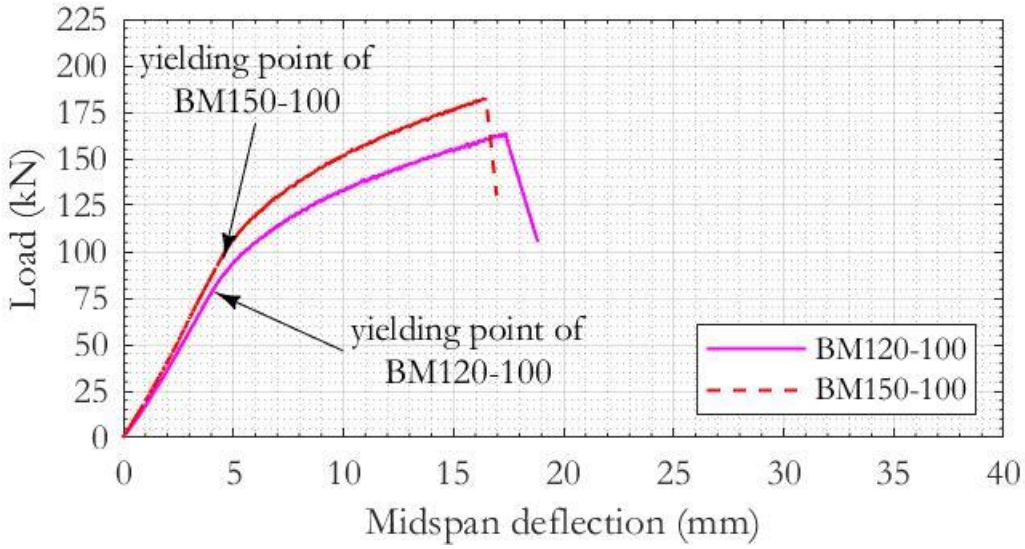

Fig. 14. Effect of FRP bond length on load-deflection curve.

3.4. Effect of Pre-damage of Steel Beam on Flexural Properties

A comparison between BM120-100 and BM120Y-100 reflects the effect of condition of the steel beam before strengthened with the CFRP plate. Figure 15 compares the load-deflection relationships between both beams. The strengthening scheme was more effective for the pre-damaged (pre-yielded) steel beam than the undamaged one. The stiffness, strength, and ductility index of the FRP-strengthened pre-damaged beam was higher than FRP-strengthened undamaged beam by 19%, 21%, and 22%, respectively. The improvement of strength, stiffness, and ductility index of the pre-damaged beam over the undamaged beam could be caused by the attained residual stains due to the pre-damage. The results are based on the beam that was preloaded until the measured bottom flange strain at midspan section was 9.7 times the yield strain of the steel beam.

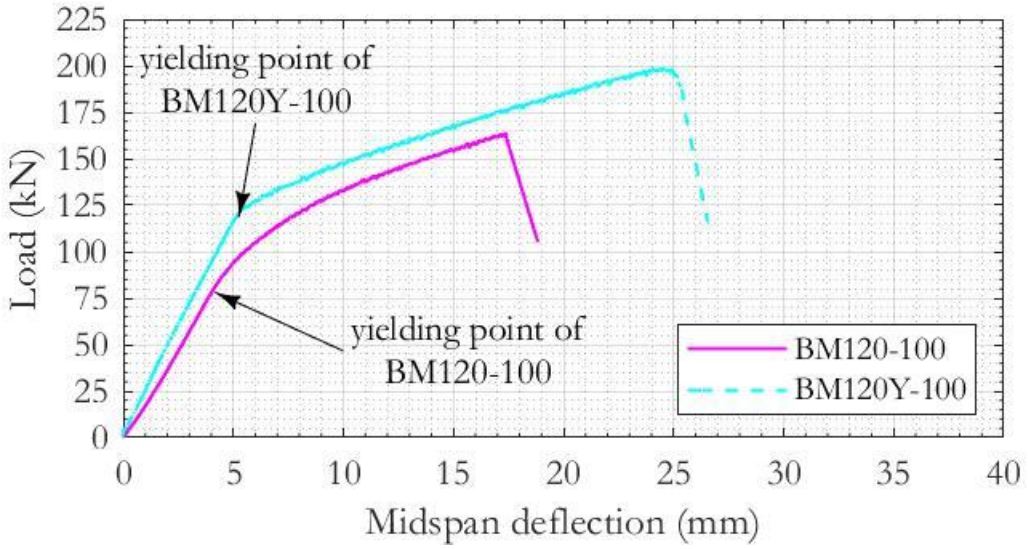

Fig. 15. Effect of pre-damage on load-deflection curve.

4. Conclusions

In this research, the effects of initial bond defect size introduced in the constant moment region, FRP modulus, length of the FRP plate, and condition of the steel beam before installation of the FRP plate (undamaged and pre-yielded conditions) on the flexural properties of CFRP-strengthened steel beams were investigated. The main conclusions are as follows,

(1) Without an initial bond defect, the failure mode of CFRP-strengthened steel beams was the FRP plate rupture. The FRP plate was effective on enhancing the maximum load carrying capacity of the steel beam by 23 to 37%. A lower modulus plate was more effective than the higher modulus one in terms of load capacity and ductility index. However, it was less effective for stiffness enhancement.

(2) The presence of an initial bond defect changed the failure mode of the FRP-strengthened steel beam from FRP rupture to intermediate debonding. The CFRP-strengthened steel beam with an initial bond defect showed an increased maximum load capacity and ductility index. Compared to the strengthened beams without the initial bond defect, the maximum load capacities were enhanced by 10 to 17%, while ductility indexes were enhanced by 17 to 61%.

(3) For the strengthened beams having the same initial bond defect size, the use of longer FRP plate increased the yield load, maximum load, and stiffness by 13%, 11%, and 12%, respectively, but decreased the ductility index by 6%.

(4) More pronounced strengthening effects on the stiffness, strength, and ductility were observed on the pre-damaged steel beam, of which the bottom flange had yielded before installation of the CFRP plate, than the undamaged one.

Acknowledgements

This research was supported by the 100th Anniversary Chulalongkorn University Fund for Doctoral Scholarship and the 90th Anniversary of Chulalongkorn University Fund (Ratchadaphiseksomphot Endowment Fund). The authors would also like to acknowledge Sika Thailand, Ltd., and Retrofit Structure Specialist, Ltd., for providing and installing FRP materials and adhesive system.

References

[1] A. H. Al-Saidy, F.W. Klaiber, and T.J. Wipf, "Repair of steel composite beams with carbon fiber-reinforced polymer plates," *Journal of Composites for Construction*, vol. 8, no. 2, pp. 163–172, 2004.

[2] X. L. Zhao and L. Zhang, "State-of-the-art review on FRP strengthened steel structures," *Engineering Structures*, vol. 29, pp. 1808-1823, 2007.

[3] H. B. Liu, R. Al-Mahaidi, and X. L. Zhao, "Experimental study of fatigue crack growth behaviour in adhesively reinforced steel structures," *Composite Structures*, vol. 90, no. 1, pp. 12–20, 2009.

[4] H. T. Wang, G. Wu, and J. B. Jiang, "Fatigue behavior of cracked steel plates strengthened with different CFRP systems and configurations," *Journal of Composites for Construction*, vol. 20, no. 3, p. 04015078, 2015.

[5] T. C. Miller, M. J. Chajes, D. R. Mertz, and J. N. Hastings, "Strengthening of a steel bridge girder using CFRP plates," *Journal of Bridge Engineering*, vol. 6, pp. 514-522, 2001.

[6] J. G. Teng, T. Yu, and D. Fernando, "Strengthening of steel structures with fiber-reinforced polymer composites," *Journal of Constructional Steel Research*, vol. 78, pp. 131-143, 2012.

[7] D. Schnerch, K. Stanford, E.A. Sumner, and S. Rizkalla, "Strengthening steel structures and bridges with high-modulus carbon fiber–reinforced polymers," *Journal of the Transportation Research Board*, vol. 1892, pp. 237–245, 2004.

[8] A. Lenwari, T. Thepchatri, and P. Albrecht, "Flexural response of steel beams strengthened with partial-length CFRP plates," *Journal of Composites for Construction*, vol. 9, no. 4, pp. 296-303, 2005.

[9] J. Deng and M. M. K. Lee, "Behaviour under static loading of metallic beams reinforced with a bonded CFRP plate," *Composite Structures*, vol. 78, pp. 232–242, 2007.

[10] M. H. Seleem, I. A. Sharaky, and H. E. M. Sallam, "Flexural behavior of steel beams strengthened by carbon fiber reinforced polymer plates - Three dimensional finite element simulation," *Materials and Design*, vol. 31, pp. 1317-1324, 2010.

[11] Y. J. Kim and G. Brunell, "Interaction between CFRP-repair and initial damage of wide-flange steel beams subjected to three-point bending," *Composite Structures*, vol. 93, pp. 1986–1996, 2011.

[12] H. Zhou, T. L. Attard, Y. Wang, J. A. Wang, and F. Ren, "Rehabilitation of notch damaged steel beams using a carbon fiber reinforced hybrid polymeric-matrix composite," *Composite Structures*, vol. 106, pp. 690–702, 2013.

[13] J. G. Teng, D. Fernando, and T. Yu, "Finite element modelling of debonding failures in steel beams flexurally strengthened with CFRP laminates," *Engineering Structures*, vol. 86, pp. 213–224, 2015.

[14] L. D. Lorenzis, D. Fernando, and J. G. Teng, "Coupled mixed-mode cohesive zone modeling of interfacial debonding in simply supported plated beams," *International Journal of Solids and Structures*, vol. 50, pp. 2477–2494, 2013.

[15] J. Deng, Y. Jia, and H. Zheng, "Theoretical and experimental study on notched steel beams strengthened with CFRP plate," *Composite Structures*, vol. 136, pp. 450–459, 2016.

[16] H. E. M. Sallam, S. S. E. Ahmad, A. A. M. Badawy, and W. Mamdouh, "Evaluation of steel I-beams strengthened by various plating methods," *Advances in Structural Engineering*, vol. 9, no. 4, pp. 535–544, 2006.

[17] H. E. M. Sallam, A. A. M. Badawy, A. M. Saba, and F.A. Mikhail, "Flexural behavior of strengthened steel-concrete composite beams by various plating methods," *Journal of Constructional Steel Research*, vol. 66, pp. 1081-1087, 2010.

[18] Y. J. Kim and A. H. Kent, "Predictive response of notched steel beams repaired with CFRP strips including bond-slip behavior," *International Journal of Structural Stability and Dynamics*, vol. 12, no. 1, pp. 1–21, 2012.

[19] J. G. Teng, T. Yu, and D. Fernando, "Strengthening of steel structures with fiber-reinforced polymer composites," *Journal of Constructional Steel Research*, vol. 78, pp. 131-143, 2012.

[20] K. Nozaka, C. K. Shield, and J. F. Hajjar, "Effective bond length of carbon-fiber-reinforced polymer strips bonded to fatigued steel bridge I-girders," *Journal of Bridge Engineering*, vol. 10:2, pp. 195-205, 2005.

[21] C. E. Chalioris, P. M. K. Kosmidou, and N. A. Papadopoulos,, "Investigation of a new strengthening technique for RC deep beams using carbon FRP ropes as transverse reinforcements," *Fibers*, vol. 6, no. 3, p. 52, 2018.

[22] B. El-Taly, "Repairing steel beams with different notch levels using composite materials," *Asian Journal of Civil Engineering*, vol. 19, no. 2, 2018.

[23] E. C. Karam, R. A. Hawileh, T. El-Maaddawy, and J. A. Abdallaa, "Experimental investigations of repair of pre-damaged steel-concrete composite beams using CFRP laminates and mechanical anchors," *Thin-Walled Structures*, vol. 112, pp. 107–117, 2017.

[24] E. Kaya, C. Kütan, S. Sheikh, and A. İlki, "Flexural retrofit of support regions of reinforced concrete beams with anchored FRP ropes using NSM and ETS methods under reversed cyclic loading," *Journal of Composites for Construction*, vol. 21, no. 1, p. 04016072, 2016.

[25] A. M. I. Sweedan, M. M. A. Alhadid, and K. M. El-Sawy, "Experimental study of the flexural response of steel beams strengthened with anchored hybrid composites," *Thin-Walled Structures*, vol. 99, pp. 1-11, 2016.

[26] A. M. I. Sweedan, K. M. El-Sawy, and M. M. A. Alhadid, "Interfacial behavior of mechanically anchored FRP laminates for strengthening steel beams," *Journal of Constructional Steel Research*, vol. 80, pp. 332-345, 2013.

[27] H. Zhou, T. L. Attard, Y. Wang, J.-A. Wang, and F. Ren, "Rehabilitation of notch damaged steel beams using a carbon fiber reinforced hybrid polymeric-

matrix composite," *Composite Structures*, vol. 106, pp. 690-702, 2013.

[28] A. Hasnat, M. M. Islam, and A. F. M. S. Amin, "Enhancing the debonding strain limit for CFRP-strengthened RC beams using U-Clamps: Identification of design parameters," *Journal of Composites for Construction*, vol. 16, p. 04015039, 2015.

[29] R. A. Hawileh, H. A. Rasheed, J. A. Abdalla, and A. K. Al-Tamimi, "Behavior of reinforced concrete beams strengthened with externally bonded hybrid fiber reinforced polymer systems," materials and design, vol. 53, pp. 972-982, 2014.

[30] L. Ombres, "Structural performances of reinforced concrete beams strengthened in shear with a cement based fiber composite material," *Composite Structures*, vol. 122, pp. 316–329, 2015.

[31] A. S. D. Salama, R. A. Hawileh, and J. A. Abdalla, "Performance of externally strengthened RC beams with side-bonded CFRP sheets," *Composite Structures*, vol. 18, pp. 32184-6, 2019.

[32] *Standard Test Methods and Definitions for Mechanical Testing of Steel Products*, ASTM A370-17a, American Society for Testing and Materials (ASTM), 2017.

[33] Sika (Thailand) Limited. (2017). *Product Data Sheet: Sikadur®-30* [Online]. Available: https://tha.sika.com/dms/getdocument.get/c421a0fc-54d0-3dfb-b213-922efcc2f307/Sika%20PDS_E_Sikadur%20-30.pdf [Accessed: Jan. 2017]

[34] J. Deng, J. Li, Y. Wang, and W. Xie, "Numerical study on notched steel beams strengthened by CFRP plates," *Construction and Building Materials*, vol. 163, pp. 622–633, 2018.

[35] O. H. Elkhabeery, S. S. Safar, and S. A. Mourad, "Flexural strength of steel I-beams reinforced with CFRP sheets at tension flange," *Journal of Constructional Steel Research*, vol. 148, pp. 572–588, 2018.

[36] J. He and G. Xian, "Debonding of CFRP-to-steel joints with CFRP delamination," Composite Structures, vol. 153, pp. 12–20, 2016.

[37] A. H. Korayem, C. Y. Li, Q. H. Zhang, X. L. Zhao, and W. H. Duan, "Effect of carbon nanotube modified epoxy adhesive on CFRP-to-steel interface," *Composites Part B: Engineering*, vol. 79, pp. 95-104, 2015.

[38] C. Li, L. Ke, J. He, Z. Chen, and Y. Jiao, "Effects of mechanical properties of adhesive and CFRP on the bond behavior in CFRP-strengthened steel structures," *Composite Structures*, vol. 211, pp. 163–174, 2019.

[39] H. T. Wang, G. Wu, Y. T. Dai, and X. Y. He, "Determination of the bond–slip behavior of CFRP-to-steel bonded interfaces using digital image correlation," *Journal of Reinforced Plastics and Composites*, vol. 35, no. 18, pp. 1353-1367, 2016.

[40] H. T. Wang, G. Wu, Y. T. Dai, and X. Y. He, "Experimental study on bond behavior between CFRP plates and steel substrates using digital image correlation," *Journal of Composites for Construction*, vol. 20, no. 6, p. 04016054, 2016.

[41] *Preparation of Steel Substrates before Application of Paints and Related Products — Visual Assessment of Surface Cleanliness—Part 1: Rust Grades and Preparation Grades of Uncoated Steel Substrates and of Steel Substrates after Overall Removal of Previous Coatings*, EN ISO 8501-1, European Committee for Standardization, 2007.

[42] H. T. Choi, J. S. West, and K. A. Soudki, "Analysis of the flexural behavior of partially bonded FRP strengthened concrete beams," *Journal of Composite for Construction*, vol. 12, pp. 375-386, 2008.

Tosporn Prasertsri, photograph and biography not available at the time of publication.

Akhrawat Lenwari, photograph and biography not available at the time of publication.

Thaksin Thepchatri, photograph and biography not available at the time of publication.